Computational Materials Science 232 (2024) 112667

Contents lists available at ScienceDirect

Computational Materials Science

journal homepage: www.elsevier.com/locate/commatsci

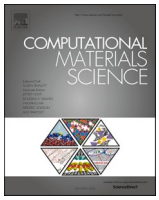

Role of atomistic modeling in bioinspired materials design: A review

Ning Zhang

Department of Mechanical Engineering, Baylor University, Waco, TX 76706, USA

ARTICLE INFO

Keywords:
Biomaterial
Atomistic modeling
Nacre
Wood
Coconut Endocarp

ABSTRACT

Biological materials have consistently intrigued researchers due to their remarkable properties and intricate structure–property-function relationships. Deciphering the pathways through which nature has bestowed its exceptional properties represents a complex challenge. The hierarchical architectures of biomaterials are recognized as the basis for mechanical robustness. Moreover, it is well-established that the intriguing properties of biomaterials arise primarily from the architecture at the nanoscale, particularly the abundant carefully designed interfaces. Driven by the diverse functionality and the increasing comprehension of the underlying design mechanisms in biomaterials, substantial endeavors have been directed toward emulating the architectures and interactions in synthetic materials. By reviewing atomistic modeling of nacre, wood, and coconut endocarp, in this work, we aim at highlighting the significant role of atomistic modeling in revealing nanoscale strengthening and toughening mechanisms of biomaterials, subsequently advancing the development of bio-inspired material.

1. Introduction

The bulk of Earth's biological materials are essentially constructed upon a few base substances including minerals, proteins, and polysaccharides [1]. With these very limited base materials, natural organisms create large varieties of structures to fulfill their diverse functions, basically confronting the challenges of life. Biomaterials are frequently encountered as intricated composites, showcasing enhanced properties in comparison to their inherently weaker individual components. Several examples include the super tough nacre, lightweight yet strong coconut shell, and extremely strong and tough spider silk. Given this inspiration, several questions are raised from both scientific and engineering perspectives. How does the natural organism attain its multifunctionality through cheap base materials? How can structural biomaterials retain the required mechanical performance? Can we use the complex structure of biomaterials to make materials with exceptional properties?

Bioinspired materials design, as a relatively young and vibrant field, aims at transferring biological principles into technically applicable base materials to foster novel solutions across different domains, which often exhibit unexpected combinations of properties [2]. The difficulty lies in discerning the mechanisms responsible for bestowing these superior properties, as well as uncovering the pathways that nature fabricates these bio-composites. The elements of biomaterials usually take shape and arrange themselves at the nanoscale. It has been widely recognized that the intriguing characteristics of natural materials arise primarily from their nanoscale structure, particularly the interfaces [3]. In spite of the substantial efforts dedicated to designing materials employing macroscopic or microscopic engineering approaches to attain desired mechanical properties [4], understanding the nanoscale structure and interfacial interactions is fundamental to most bioinspired materials design.

With cutting-edge methodologies, achieving comprehensive measurements of the interfacial properties and decoding of the associated mechanisms at the nanoscale or atomic scale solely through experimental techniques are extremely challenging, even not possible. To a certain degree, scanning electron microscope (SEM) and atomic force microscopy (AFM) possess the ability to quantify and visualize interfaces at a finer scale. However, major roadblocks exist in such techniques, including considerations of instrument resolution and sensitivity, as well as the preservation of sample integrity during preparation and testing [3]. Moreover, the nanoscale interactions surpass the detection capabilities of existing experimental methodologies. As a result, the exact material configurations of some biomaterials, such as the cell wall of coconut endocarp, are still under debate or unexplored. Although researchers frequently attribute the excellent mechanical properties of biomaterials to the so-called "nano effects", direct experimental evidence at the nanoscale remains scarce, primarily due to the encountered challenges.

Furthermore, the mechanical response of biomaterials is notably

E-mail address: ning_zhang@baylor.edu.

https://doi.org/10.1016/j.commatsci.2023.112667
Received 5 August 2023; Received in revised form 19 November 2023; Accepted 20 November 2023
Available online 28 November 2023

influenced by the water absorbed within their organic matrix. Experimental investigations, particularly those highlighting the remarkable toughness of nacre [5,6], predominantly conducted under hydration conditions, demonstrate the pivotal role of water. Experimental observations indicate that water-induced changes in the shear modulus and strength of the organic matrix are key factors affecting the elastic modulus, tensile strength and toughness of nacre [7]. Moreover, the presence of water at nanograin interfaces adds to the viscoelastic nature of nacre [8,9]. Regarding cellular plant materials, a nanoindentation study focused on wood [10] has unveiled that water molecules permeate the ultrastructure of the wood cell wall, serving as a softening agent. This subsequently leads to a decrease in both hardness and elastic moduli of wood. Despite the availability of advanced experimental techniques for precisely assessing the impact of water on the mechanical properties of biomaterials, the intricate fundamental mechanisms by which water facilitates them in achieving their anticipated properties remain elusive, especially at the fine scale.

To address the challenges posed by experimental limitations, computational modeling, particularly atomistic modeling, has been grown into a viable technique to replicate the dynamic behavior of materials exposed to different loading scenarios at the nanoscale. In this work, several studies of biological materials will be taken as examples to manifest the role of atomistic modeling in advancing the development of bioinspired materials. We will focus on two representative categories: hard biomineral and biomass cellular materials. Firstly, the enduring fascination with biominerals such as nacre and bone stems from their exceptional synergy of high strength, stiffness, and toughness, along with their versatile nature and inherent capacity for self-repair. The path often adopted by nature involves incorporating submicron- or nano-sized mineral platelets into a soft organic matrix, establishing a thoughtfully arranged hierarchical structure. The crucial aspect lies in the generation of abundant interfaces between organic and inorganic components plus the harness of the synergistic mechanisms that operate at various scales to disperse loads, absorb energy, mitigate damage, as well as withstand property changes due to occurrences like cracking. Secondly, the prospect of sustainable development is closely tied to humanity's capacity to transition away from exhaustible fossil reserves to renewable and eco-friendly alternatives. Encompassing more than 30 % of the world's land surface, the forest bestows upon humanity one of nature's most generous offerings. It serves as a habitat and a valuable source of materials for countless living creatures [11]. The intrigue surrounding wood and its derivatives stems not only for being sustainable, renewable, and biodegradable but also for their impressive mechanical properties and adaptable chemistry.

The intention of this article is to provide additional insights into the numerous high-quality reviews on the overarching topic of bioinspired materials design [1–3]. A significant portion of the content is dedicated to evaluating the endeavors in atomistic modeling of nacre, wood and coconut endocarp, placing special emphasis on their mechanical behavior study. Specific attention is given to deciphering how interfacial mechanics influence the overall holistic mechanical characteristics of biomaterials, opening up potential applications in the realm of bioinspired engineering. Lastly, we engage in an in-depth analysis of the constraints inherent to atomistic modeling. Furthermore, we lay out prospects for future research exploration.

2. Nacre

The iridescent layer found within mollusk shells, commonly referred to as nacre or mother-of-pearl, is of significant interest. The principal role of nacre is to provide protection to the shell, mitigating the risk of catastrophic fractures induced by predator assaults [6]. It has been widely acknowledged for an extended period as the foremost natural material for armor [12]. Assessed from the standpoint of fracture mechanics, biominerals consistently excel in enhancing fracture resistance during crack propagation compared to engineered synthetic materials. This superiority is owed to the utilization of toughening mechanisms operating both in front of and behind the crack tip.

The structure of nacre exhibits a highly intricate hierarchical organization that spans various length scales, ranging from the atomic scale to the macroscale, as illustrated in Fig. 1 [13]. Microscale structure analysis reveals that nacre predominantly comprises polygonal aragonite platelets that account for roughly 95 wt% of its composition. The dimensions of these platelets are defined by their width, which ranges from 10 to 20 μm, and their thickness, measuring about 0.5 μm. Interweaved between these platelets are delicate layers of organic protein and polysaccharides matrix, serving as the "relatively soft" adhesive material, situated at the interfaces between mineral platelets [14]. Through such a clever assembly strategy, nacre acquires a noteworthy three-thousand times augmentation in fracture toughness with a marginal compromise in strength in comparison to the pure mineral phase, notwithstanding its predominant composition [7,15].

Leveraging the high-resolution transmission electron microscopy (TEM), it was additionally unveiled that each aragonite tablet involves the integration of nanograins, varying in size from 3 to 10 nm, that are intricately associated with proteins such as lustrin A [16], perlucin [17], perlustrin [18], and perlwapin [19], embedded in the grain boundaries (GBs) [20]. This discovery refreshes the long-term accepted conventional assumption of single crystalline aragonite tablets, and furthermore, it provides a potential toughening nature to complement the ever-reported mechanisms that mainly focused on the structure of microscale laminates, including tablet sliding [21,22], interfacial asperities [21], mineral bridges [23–25], and interlock of wavy tablets [5]. Besides, soft biopolymer fibers, mainly chitin, were found to glue the hard aragonite tablet together, which was demonstrated to contribute significantly to energy dissipation during deformation and hence high fracture toughness of nacre [26,27]. These efforts have greatly improved our understanding of the structure-composition-performance relationships of nacre. However, unfortunately, they were still incapable of fully interpreting the dramatic enhancement (~3000 times increase) of the toughness in nacre. With this concern in mind, a variety of research endeavors have been executed to comprehend the mechanisms that contribute to the enhanced toughness of nacre tablets [13,28]. Studies have revealed that the ionic cross-linking of densely folded macromolecules within the nano tablet is of equivalent importance. Upon loading, the protein chains were stretched in a sequential manner as folded domains were gradually unfastened. This stepwise elongation process could potentially contribute to the astounding toughness attributes exhibited by nacre [28].

The optimal approach for achieving a profound understanding of the molecular interactions between mineral and organic molecules is through a comprehensive inquiry into individual constituents and their collective composite. This will elucidate the distinct functions of diverse nacre components, thereby offering insights for enhancing the performance of materials derived from nacre.

2.1. Aragonite

Aragonite embodies a metastable form within the calcium carbonate crystal family, rendering it one of the most prevalent biomineral due to its substantial production levels and its wide-ranging dispersion. Considering its predominant composition in nacre, it becomes imperative to examine aragonite both in single crystalline and polycrystalline forms when it is subjected to various loading conditions. By doing so, we can simulate their response to external attacks that nacre might experience. Gaining insights into the deformation mechanisms within aragonite is vital for grasping the overall exceptional mechanical performance of nacre.

Through nanoindentation and uniaxial compression simulations of single crystalline aragonite [29], we examined their mechanical properties and associated deformation mechanisms. These simulations aimed to emulate the real-life predatory penetrating impacts that nacre

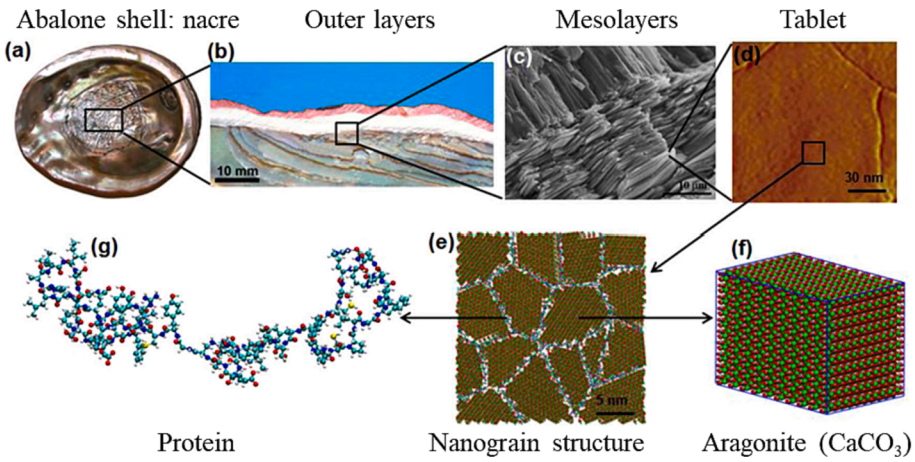

Fig. 1. The structured hierarchy observed in abalone shell nacre [13].

commonly faces within marine environments, often occurring under significantly elevated strain rates. The primary outcome of this research underscores the substantial role played by crystallographic orientations and loading rates in shaping the mechanical responses of aragonite, namely its hardness, stiffness and strength.

The load–displacement curves (Fig. 2a) exhibit rather different patterns when indenting along different directions. The hardness along [0 0 1] direction was calculated as 9.04 GPa, which closely aligns with the experimental result of 8.6 ± 0.36 GPa [30]. In contrast, the hardness measured along the [100] direction yielded a value of 7.96 GPa, which further supports the experimental conclusion [31] that (0 0 1) plane possesses greater hardness than other planes within aragonite. Atomic configurations analysis revealed that in the case of [100]-indentation, a new regularly arranged phase formed around the local compressed area (Fig. 2b). Conversely, when indenting along the [0 0 1] direction, an adjacent pileup region became evident, as depicted in Fig. 2c. This occurrence bears resemblance to the observations reported in experimental studies [30]. No dislocations or cracks were detected. Retrieving the load–displacement relationships in Fig. 2a, one may conclude that the pileup zone formation in the [0 0 1]-indentation case implies tardy energy release and subsequent high hardness. On the other hand, in the case of [100]-indentation, the initiation and expansion of the new phase mitigate stress concentration and are accountable for the decrease in the hardness of the bulk aragonite.

Analogous crystallographic orientation effect was observed when uniaxially compressing a cubic aragonite model with 2.37 million atoms (Fig. 3a). The stress plateaus were observed in both cases indicating a stable energy release process. The calculated Young's modulus, i.e., stiffness, of [0 0 1]-oriented aragonite reaches 80 GPa, which is comparable to the experimental measurement of 82 GPa [32]. However, when compressed along [100] direction, a relatively smaller stiffness of 67 GPa was obtained. Besides, significant decreases in yield strength and strain were observed when altering the loading direction from [0 0 1] to [100], i.e., 6.0 GPa vs. 1.6 GPa, and 8 % vs. 2 %, respectively. Snapshots of the deformed structure revealed that in the [100]-oriented case, dislocation first nucleate and propagate, followed by new phase transformation and deformation twinning, as demonstrated in Fig. 3b, c. The transformed phase displays symmetry with the twin boundaries, manifesting an inclination angle of 68.2^0, which aligns closely with an experimentally reported value of 63.8^0 [12], nevertheless, no phase transformation was reported experimentally. As for the compression along [0 0 1] direction, the stress plateau after yielding is ascribed to a uniform atomic structure arrangement. Thereafter, a catastrophic failure happens along the (1 1 0) and ($\bar{1}$10) slip planes.

The results from indentation and compression confirm that (0 0 1) is harder and stronger than the (1 0 0) plane. From this viewpoint, one can appreciate the rationale behind nacre's formation of the "brick-and-mortar" structure, wherein the [100] axis of aragonite is positioned vertically to the surface, providing protection against aggressive predatory penetrating attack.

Brittle materials, such as ceramics, glass and minerals, commonly exhibit abrupt fracture as their primary mode of failure. Hence, it

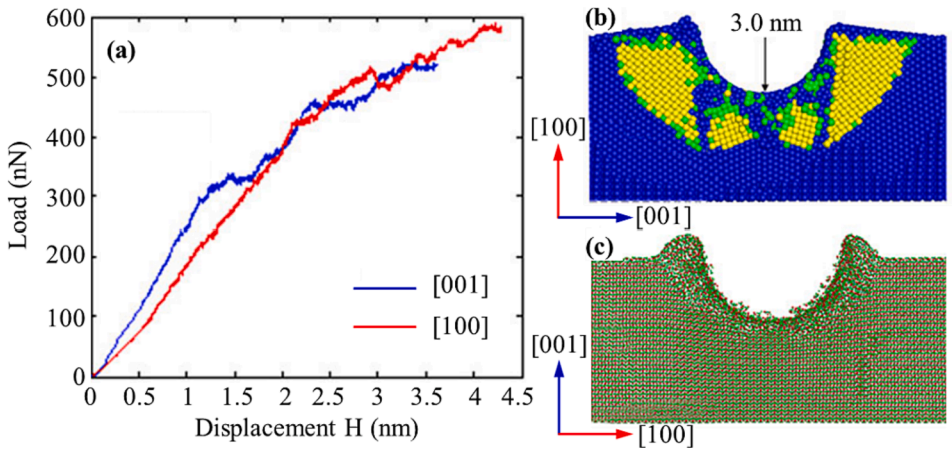

Fig. 2. (a) Crystallographic orientation effect on load–displacement curves of nanoindentation on aragonite. (b) Phase transformation induced by indentation along [100] direction. The original aragonite phase is denoted by blue atoms, the new phase by yellow atoms, and the amorphous phase by green atoms. (c) Atoms beneath and surrounded the indenter form pile up when indenting along [0 0 1] direction [29].

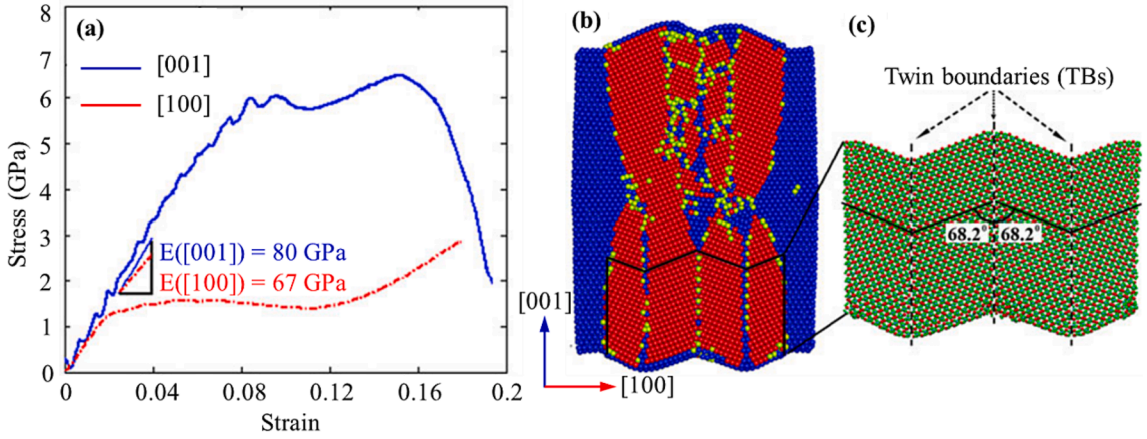

Fig. 3. (a) Crystallographic orientation effect on stress–strain curves of uniaxial compression on aragonite. (b) Phase transformation and deformation twinning induced by compression along [100] direction. Blue, red, and yellows atoms denote the original aragonite phase, new phase, and amorphous phase, respectively. (c) Atomic configuration of the deformation induced twinning [29].

becomes imperative to examine the manner in which cracks propagate in aragonite. Given that crack initiates and propagates at the nano or atomic level, operating on a fleeting picosecond timeframe, they exceed the capabilities of both experimental and continuum-level simulation approaches. Alternatively, atomistic modeling is powerful in investigating bond breaking, crack surface formation, and the crack propagation path [33,34].

Molecular dynamics (MD) technique was adopted to investigate the dynamic fracture behavior of single-crystalline aragonite [34]. Given the discrepancy in ionic interactions between (1 0 0) and (0 1 0) planes, and the similarity in crystal structure between (0 1 0) and (1 1 0) planes, as evidenced in Fig. 4a, two specific crack types were deliberately introduced along the [0 1 0] and [100] directions within the modeled systems. Crack deflection and straight propagation were observed in these two cases, respectively, as captured in Fig. 4b, c. The primary outcome of this study is the discernment that crack propagation in aragonite predominantly occurs along the (1 1 0) and (0 1 0) planes, thereby offering insights into the interpretation of its relative behaviors in terms of ductile and brittle fracture.

2.2. Protein – Aragonite interaction

It is postulated that the organic matrix plays dual roles in nucleating and dictating the growth of aragonite crystals, as well as gluing the single crystalline nanograins together to endow nacre the desired mechanical performance [17,35]. Facilitated by atomic force microscopy (AFM), force–displacement curves featuring distinctive sawtooth patterns were recorded when pulling flexible proteins out of a nacre tablet. Mechanisms such as elongation of macromolecules, bonds sacrifice, and length concealment [36], particularly, protein chains unfolding, have garnered widespread acceptance as the primary source of the observed sawtooth pattern. These mechanisms substantially facilitate energy dissipation and result in the notable fracture toughness of nacre [37].

To investigate the protein – mineral interaction in nacre, it is a fundamental requirement to construct a computer model (depicted in Fig. 1e) capable of faithfully replicating the behavior of the nano tablet. However, due to the inherently pliable nature of proteins, discerning their arrangement on the irregular GBs of polycrystalline aragonite poses an exceptionally formidable task. To tackle this challenge, the steered molecule dynamic (SMD) method was adopted to drag four different types of proteins, i.e., lustrin A [16], perlucin [17], perlustrin [18], and perlwapin [19], into the pre-defined GBs [13,35]. The attained

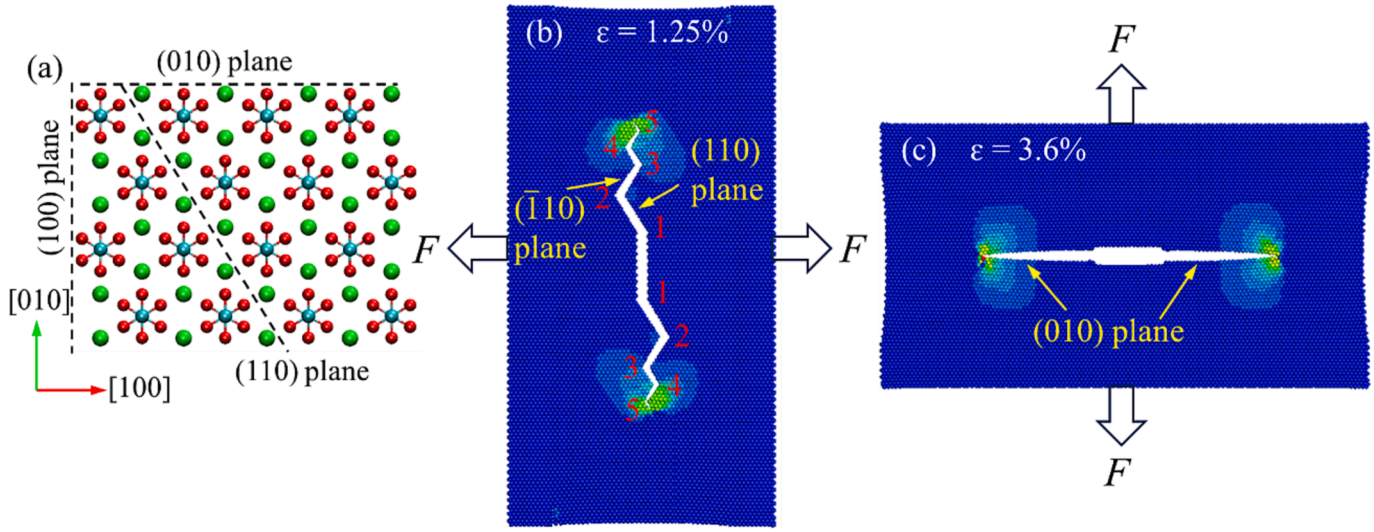

Fig. 4. (a) Aragonite crystalline structure with dash lines denote the (1 0 0), (0 1 0) and (1 1 0) planes. The propagation of cracks in aragonite with pre-existing central cracks along (b) [0 1 0] direction and (c) [100] direction. In (b) and (c), the atoms are colored based on their atomic kinetic energy [34].

force-extension curves were characterized by a sawtooth pattern (Fig. 5a), which demonstrated remarkable similarity to those observed in the AFM experiment. However, unlike the commonly acknowledged mechanisms of protein self-unfolding, the identified sawtooth behavior (Fig. 5b, c) was found to be correlated with the ionic bonding occurring between protein and aragonite, namely the electrostatic interactions. The relationship between the density of ionic bonds and the magnitude of sawtooth curves can be directly acquired from Fig. 5a. This study yielded novel perspectives on the source of the substantial energy necessary for breaking nacre. Specifically, it highlighted the potential importance of ionic electrostatic interactions at the organic–inorganic interfaces, which could be a key factor in enhancing the toughness of nacre.

The influence of water on the interaction between protein and mineral was further explored using SMD simulations. For comparison, proteins situated on GBs were studied in both dry and hydrated states. The obtained load–displacement curves (Fig. 6a) indicated that the force peaks were smoothed with the presence of water, leading to the observed force plateaus. By monitoring the atomic trajectories (Fig. 6b, c), it was observed that a layer of water formed on the mineral surface, effectively isolating the ionic interaction between the protein and mineral. Meanwhile, the introduction of water induced abundant hydrogen bonds, collectively contributing to the passivation of the observed blunt force peaks.

2.3. Biomineral composite

In a systematic effort to comprehensively uncover the toughening mechanisms operating within nacre at the nanoscale, with a specific focus on elucidating the pivotal contribution of proteins to enhancing nacre's toughness, a mineral-protein composite model was meticulously constructed through the Steered Molecular Dynamics (SMD) approach (depicted in Fig. 7a, b) [13]. The average width of GBs was controlled at 1.2 nm, which agrees well with the experimental value [27]. Water molecules were incorporated into the GBs to emulate the hydration state analogous to that observed in nacre. To provide a basis for comparison, both single crystalline and polycrystalline aragonite models were constructed to emulate the properties of pure mineral and dehydrated nacre, respectively. Uniaxial tension simulations were carried out on the three models with a relatively low strain rate of 2.0×10^7/s. The stress–strain curves obtained (depicted in Fig. 7c) display deformation patterns akin to those observed in experimental data [9]. The behavior of single crystalline aragonite is indicative of brittle fracture, featuring notable strength at 970 MPa and a significant stiffness of 75 GPa, albeit marginally lower than the values extrapolated from experimental estimates [9]. Dislocation motion and phase transformation were found to be responsible for its ultimate failure. Inelastic deformation was observed from the very beginning in the case of polycrystalline aragonite under tension. It was noted that there is a significant strength drop, which is primarily due to the weak connections on GBs.

In contrast, with the incorporation of pliable organic substances and water molecules onto the GBs, the fracture toughness modulus, as computed through integrating the stress–strain curve until the point of failure, demonstrated a substantial enhancement, as illustrated in Fig. 7c. A comprehensive analysis of atomic configurations disclosed that both nanograins and grain boundaries experienced stretching, resulting in an expansion in width, yet without undergoing catastrophic failure. The acidic and basic amino acids demonstrate a strong propensity for binding with the calcium carbonate ions, signifying a robust electrostatic interaction between them. It is a well-established fact that electrostatic interactions are significantly stronger, surpassing the strength of hydrogen bonds (H-bonds) formed within the folded protein chains by over twenty times. Given this, it is plausible to assert that ionic bonding contributes more significantly than protein self-unfolding to the high level of toughness witnessed in nacre. This discovery contributes a fresh angle to the assortment of toughening mechanisms found in nacre: the toughening triggered by robust electrostatic interactions. This strategy of toughening has been employed to manipulate the interfaces between layers when fashioning composites resembling the architecture of nacre [38].

3. Wood

Wood is arguably one of the most prevalent biomaterials worldwide. It possesses a unique set of features – pronounced porosity, lightweight nature, impressive strength, stiffness, hardness, and toughness – a combination that is scarcely encountered in artificially produced materials [39]. In terms of strength-to-weight ratio, wood competes with steel [39]. Its fracture toughness surpasses that of the majority of porous materials manufactured by humans by several orders of magnitude [40]. For centuries, the significance of wood lies in its role as both a fundamental construction material and a critical resource for making pulp and

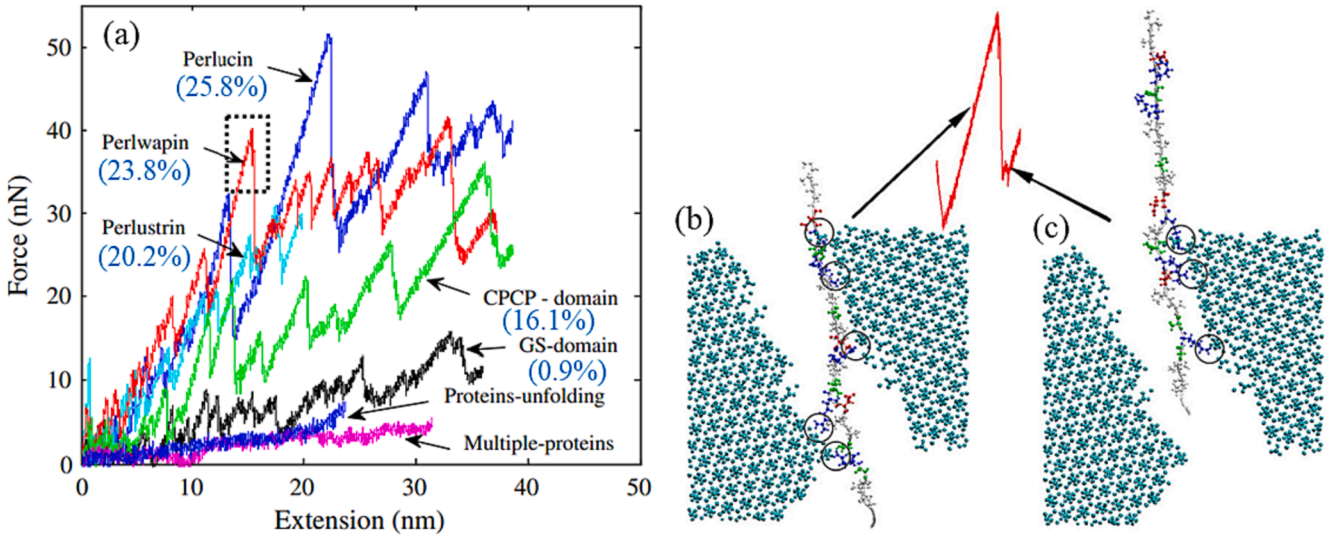

Fig. 5. (a) Force-extension curves during the extraction of protein chains from GBs, as well as from protein bundles. The density of ionic bonds for individual proteins is shown in the figure. Atomic trajectories of a specified GB region (b) before and (c) after the force peak. Different types of residue were visualized using varied colors, wherein acidic and basic amino acids were represented in red and blue, while polar and nonpolar amino acids were denoted in green and white, respectively [35].

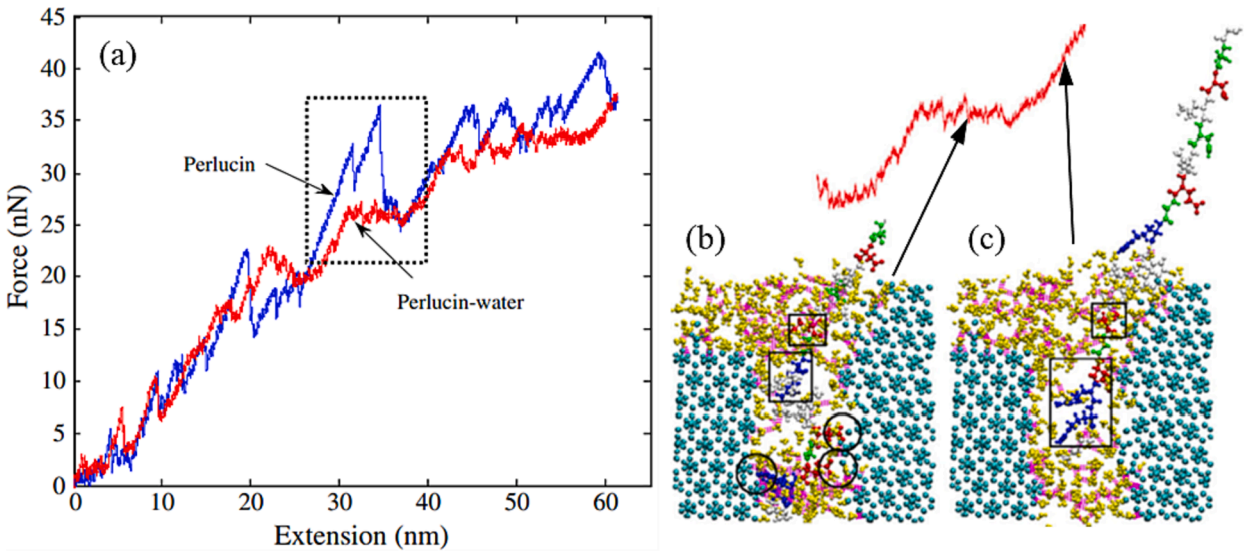

Fig. 6. (a) The effect of water on force-extension curves of perlucin-aragonite interactions. Snapshots of atomic configurations (b) at and (c) after the plateau region in the force-extension curve [35].

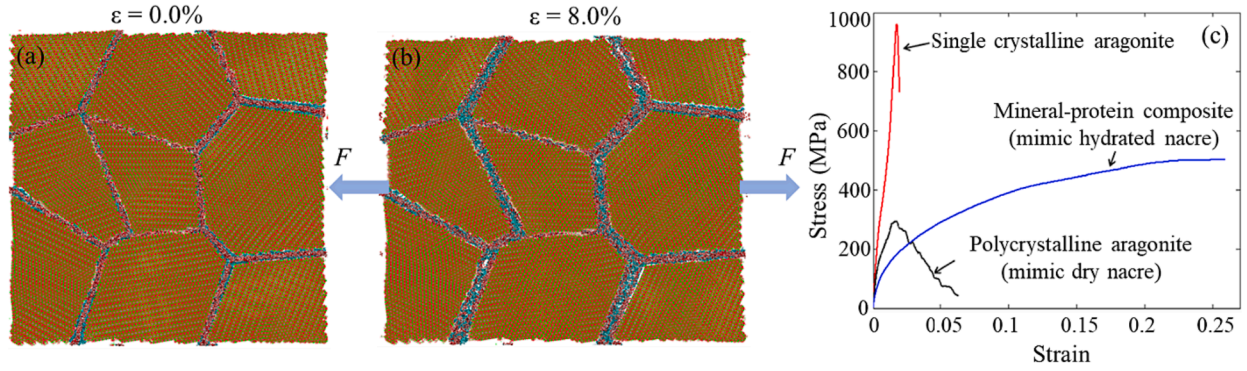

Fig. 7. Configurations of mineral-protein composites at the strains of (a) ε = 0.0 % and (b) ε = 8.0 %. (c) stress–strain responses in uniaxial tension for single-crystal aragonite, polycrystal aragonite, and mineral-protein composite. [13].

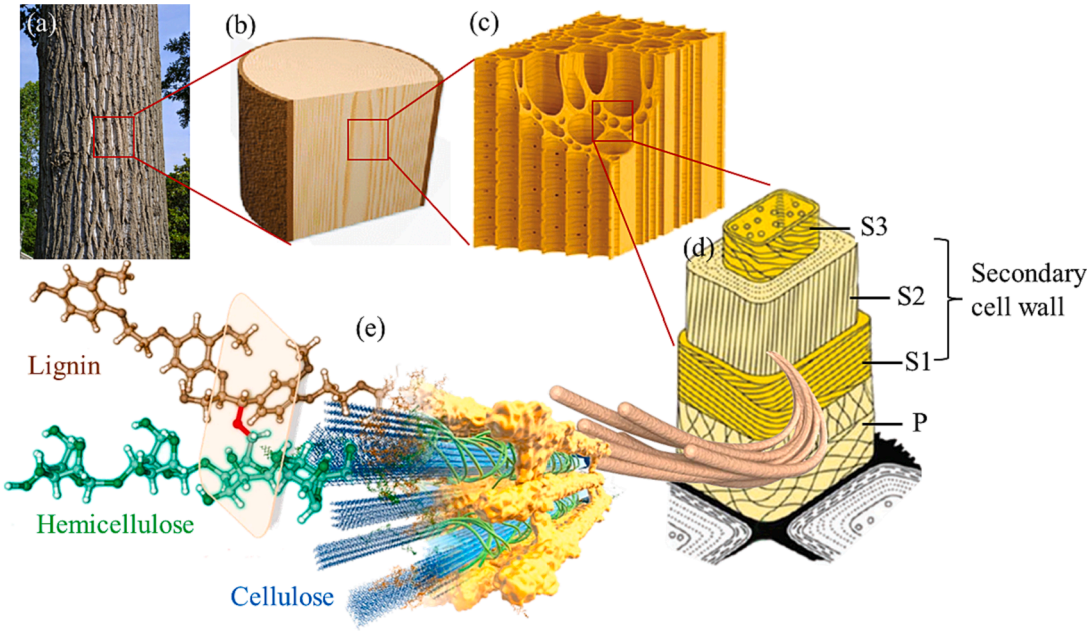

Fig. 8. The hierarchical structure of wood materials ranging from (a) tree stem, (b) wood bulk, (c) cellular structure, (d) cell wall and (e) microfibril.

paper. Emerging delignified wood (DW) scaffolds have been customized for a range of uses, including transparent wood [41,42], high-performance thermal insulation [43], energy generation technologies [44], and additional bioinspired wood products [45]. Leveraging state-of-the-art nanotechnologies, the potential of wood can be remarkably expanded, encompassing domains such as nanostructured wood membranes [46,47], carbonized wood nanocomposites [48], and the field of wastewater treatment [49].

Primary layer and secondary cell wall layers, consisting of the S1, S2, and S3 layers (as shown in Fig. 8d), constitute the primary structural elements of the wood cell wall. An essential factor contributing to the extraordinary mechanical characteristics is the substantial secondary cell wall, comprising roughly 80 % of the entire thickness, and distinguished by a sophisticated hierarchical configuration (depicted in Fig. 8). In the secondary cell wall, the S2 layer serves as a fundamental building block, creating a composite reinforced by fibers. This layer contains crystalline cellulose polymers of about 3 nm in diameter, intricately incorporated into a pliable matrix of amorphous lignin and hemicellulose, whose thickness varies between 3 and 14 nm [50,51]. Moreover, lignin occupies the interstitial spaces, confining the mobility of microfibrils and augmenting the hydrophobic characteristics of the cell wall [52]. Cellulose microfibrils exhibit a longitudinal stiffness of around 134 GPa, whereas the amorphous hemicellulose and lignin possess moduli of only 7 GPa and 2 GPa, respectively [53]. Realizing the complete capabilities of wood necessitates a comprehensive comprehension of its structural hierarchy and mechanics, particularly at the nanoscale, thereby paving a way for entirely novel nanotechnological applications.

3.1. Effect of binding mode

Hemicellulose segments were noted to establish connections with adjacent cellulose microfibrils through different binding modes [54]. To gain a better understanding of how hemicellulose binding modes affect the mechanical performance of cellulose-hemicellulose composite, atomistic shear simulations were conducted on the three models with bridging, looping and randomly distributed hemicellulose chains, as illustrated in Fig. 9a-c [55]. It is worth noting that the three models were initially designed to maintain a consistent contact area between hemicellulose and cellulose bundles, ensuring the constancy of initially formed H-bonds. The obtained shear force–displacement curves (Fig. 9d) implies that shear force is affected by the binding modes. It was noted that after full relaxation the interfacial area altered, and additional hydrogen bonding was observed on the cellulose-hemicellulose interfaces. The presence of these H-bonds is crucial in inhibiting the relative motion between cellulose and hemicellulose. Besides, the hemicellulose chain backbones underwent elongation to withstand further deformation. The strength of this covalent interaction is twenty-fold greater than the non-bonded interaction, resulting in a substantial enhancement of the composite's shear strength. Acknowledging that water serves as a significant origin of H-bond formation, there was a notable rise in the quantity of H-bonds in the aqueous environment. However, water molecules involved hydrogen bonds simply move with the polymer chains rather than strengthen the interface. Consequently, water is identified as a lubricant at the interface and plays a role in matrix softening as reported in the experimental study [56].

3.2. Effect of microfibril angle (MFA)

In the secondary layer, particularly the S2 layer, the microfibrils are parallelly oriented with different inclinations (Fig. 8d), which is measured by the MFA, denoting the angle form between the cellulose bundles and the longitudinal direction. Relatively small MFAs ($10—30^0$) were reported in the S2 layer, and it is well recognized that the mechanical performance of wood cell wall is strongly governed by the MFA [57,58]. Although prior research has involved continuum-level theoretical simulations [54,59,60] aimed at investigating the mechanical behavior of wood, they are incapable of providing the nanoscale failure mechanisms present in the wood cell wall, such as the effect of MFAs on mechanical performance. In this regard, MD simulations were conducted on hydrated cellulose-hemicellulose composite with an attempt to study the effect of MFAs (Fig. 10) [61]. Simulation results (Fig. 10a, b) accurately mirrored the experimentally identified kink bands (Fig. 10d) [61], which are assumed to be a consequence of localized buckling within the cellulose microfibril. Elastic modulus and ultimate strength decrease with the increase of MFAs (Fig. 10c). Obvious buckling and steps of cellulose bundles, detachment of hemicellulose, as well as voids were observed in the cases with big MFAs (Fig. 10b). This conclusion can be used to explain why the S2 layer always has the smallest MFAs. In addition, water was identified to exert a beneficial effect on the properties of composites featuring small MFAs.

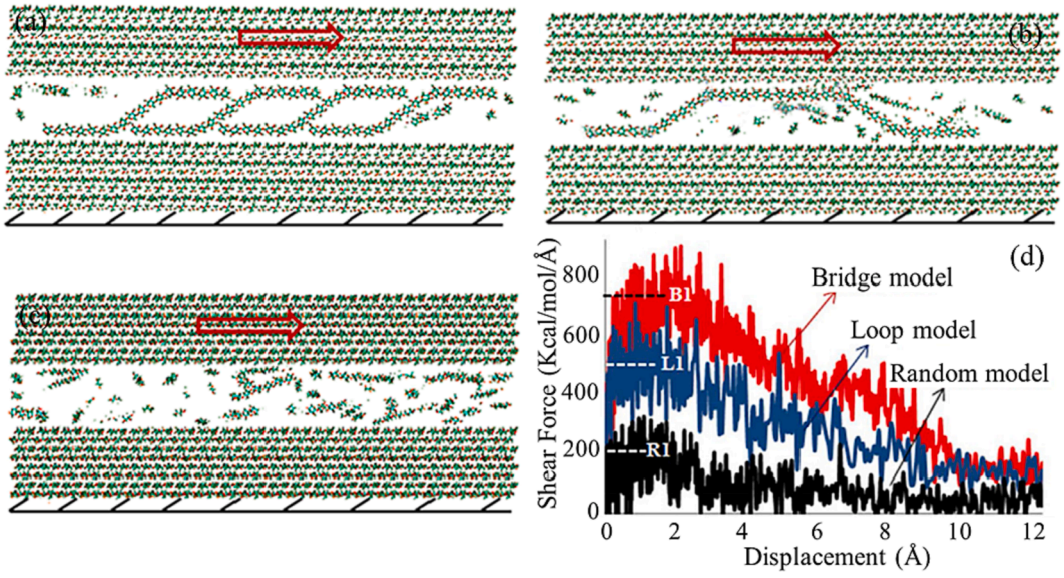

Fig. 9. Cellulose-hemicellulose composites with (a) bridging, (b) looping and (c) randomly distributed hemicellulose chains. (d) Shear force–displacement curves for the (a)-(c) models under shear [55].

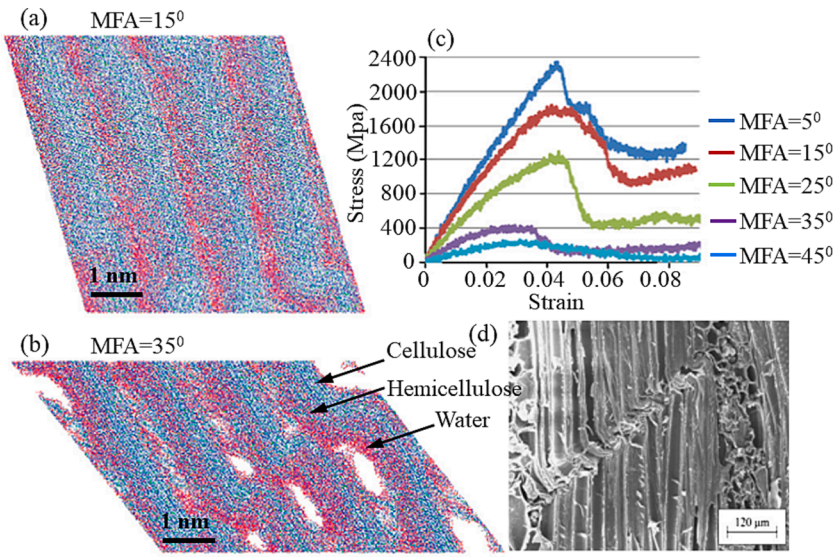

Fig. 10. Hydrated cellulose-hemicellulose composites with MFAs of (a) 15^0 and (b) 35^0 under uniaxial compression. (c) Compressive tress-strain curves of models with different MFAs. (d) Failed structure of cell wall from experiment [61].

4. Coconut endocarp

The coconut, classified as a tropical drupe, possesses a fruit wall comprising three well-defined layers: the outermost exocarp, resembling skin, the fibrous and substantial mesocarp, and the inner endocarp, which is both hard and tough (Fig. 11a). The endocarp draws our focus due to its exceptional combination of attributes—namely, the simultaneous presence of low weight, high strength, hardness, and toughness—a combination that is traditionally considered to be contradictory [62,63]. Through evolutionary processes, the architecture of the endocarp has been refined, allowing it to effectively carry out its biomechanical roles: absorbing impact when it drops from the tree, safeguarding the seed and its nourishing milk for the seedling's growth, and thwarting attempts at opening by both humans and animals.

The aged coconut endocarp contains a considerable amount of hollow vascular cell channels (Fig. 11b-d), which significantly increase its porosity. Unlike artificially engineered porous materials, the mechanical characteristics of the endocarp remain uncompromised despite its considerable porosity. The coconut endocarp exhibits a compressive strength ranging from 230 to 270 MPa [64,65], which is in line with that of mild steel (~250 MPa) [62,66]. The fracture toughness of coconut endocarp, as measured at 24.8 ± 8.4 kJ/m^2 [64], surpasses that of the majority of artificial porous or cellular materials by several orders of magnitude. For instance, porous ceramics exhibit fracture toughness levels within the range of 12.0 to 16.0 J/m^2 [67], which are significantly lower. The coconut endocarp is also widely acknowledged for its elevated hardness (500–540 MPa) [64] as well as its notable stiffness (ranging from 8.0 to 10.0 GPa) [65]. Comparatively speaking, the coconut endocarp stands head and shoulders above other natural cellular materials, including wood. With only a slightly higher density (~1.25 g/cm^3) than wood (~1.14 g/cm^3), the endocarp exhibits about ten times higher strength and fracture toughness than traditional wood tissues, such as bamboo and basal wood [68,69]. These remarkable properties, far beyond similar synthetic materials, make endocarp a great candidate for many engineering applications [70,71].

Endocarp forms a hierarchical structure (Fig. 11) with four important levels: tissue level, cell level, sub-cellular scale, nanometer, and molecular scale. As of the present, the specific nanoscale organization of cellulose, hemicellulose, and lignin within the coconut endocarp remains a subject of uncertainty. To unravel the mysteries behind the exceptional strength, toughness, and hardness of the coconut endocarp, even in the presence of significant porosity, researchers have engaged in experimental investigations centered around specific mesoscale and microscale structures, as well as mechanical properties [64,70,72].

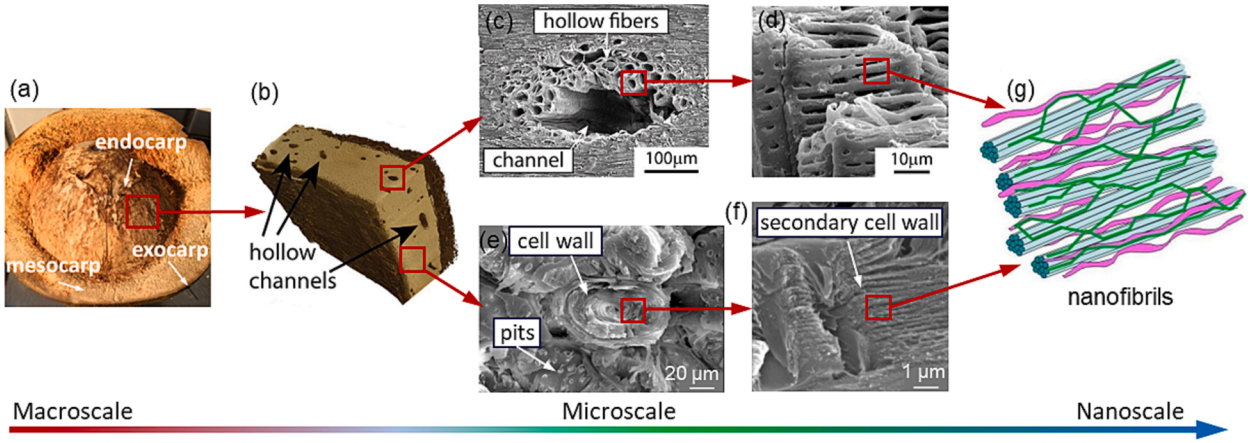

Fig. 11. The hierarchical arrangement found in coconut endocarp. (a) Coconut shells; (b) tissue level; (c-d) vascular channel and hollow fibers; (e) fracture surface of sclereid cells; (f) cell wall layers; (g) schematic cellulose nanofibrils, hemicellulose and lignin [70,72].

Nevertheless, there is a lack of comprehensive exploration into the quantitative comprehension of the mechanisms through which the coconut endocarp achieves its exceptional mechanical capabilities. Besides, nanoscale characterization of this structure and its mechanical response are missing. To date, quantitative structure-properties relationships have not been established for coconut endocarp; no one has ever produced a polymer composite that approaches the mechanical properties of the coconut endocarp by synthesis or by computer simulations.

In most cases, a material's strength originates from the nano- and sub-micrometer scales, where organic polymer chains assemble into fibrils embedded within a matrix [73,74]. In contrast, toughness is often dictated by structures at the micrometer and larger scales, where mechanisms such as crack bridging and deflection impede crack propagation [75–77]. Early investigations into understanding the mechanisms behind plastic deformation primarily employed experimental methods focused on the microscale. The suggested mechanisms for enhancing toughness have primarily concentrated on the characteristics of cell wall layers, with specific attention given to surface pits and open channels [70]. Numerical studies pertaining to coconut shells have primarily been limited to the scale of the fiber arrangement within the mesocarp [78].

In contrast to wood material where cellulose predominates, the cell wall of the endocarp features a higher lignin content, consisting of approximately 29 % cellulose, 20–30 % hemicellulose, and 44 % lignin [79–81]. Considering the pivotal significance of the interactions between diverse polymer types in shaping the comprehensive mechanical behavior of the endocarp, it becomes imperative to enhance our comprehension of the nanoscale deformation mechanisms. With this objective in mind, atomistic modeling was employed to elucidate the interplay among cellulose, hemicellulose, and lignin [82]. Through SMD shear simulations on interconnected polymer chains, it was determined that the interactions between cellulose and hemicellulose displayed the highest interfacial strength, while the interactions between cellulose and lignin exhibited the lowest interfacial strength (as depicted in Fig. 12). This disparity is ascribed to the variation in oxygen density among the components, with cellulose (27.6 %), hemicellulose (24.2 %), and lignin (10.5 %), as oxygen serves as the acceptor during hydrogen bond formation.

Through uniaxial shear and tension simulations performed on polymer composites confined between layers (as illustrated in the insets of Fig. 13), it is confirmed that cellulose–hemicellulose–cellulose

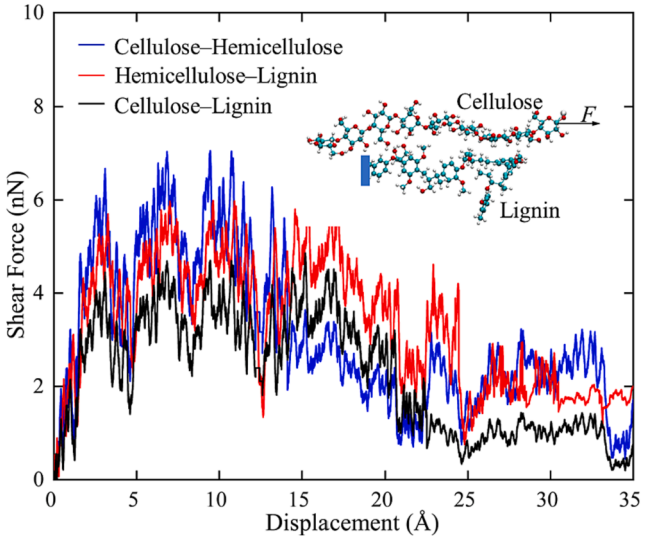

Fig. 12. Force-displacement curves from SMD shear simulations, offering insights into the interactions of cellulose–hemicellulose, hemicellulose–lignin, and cellulose–lignin pairs. The inset describes a representative pair model [82].

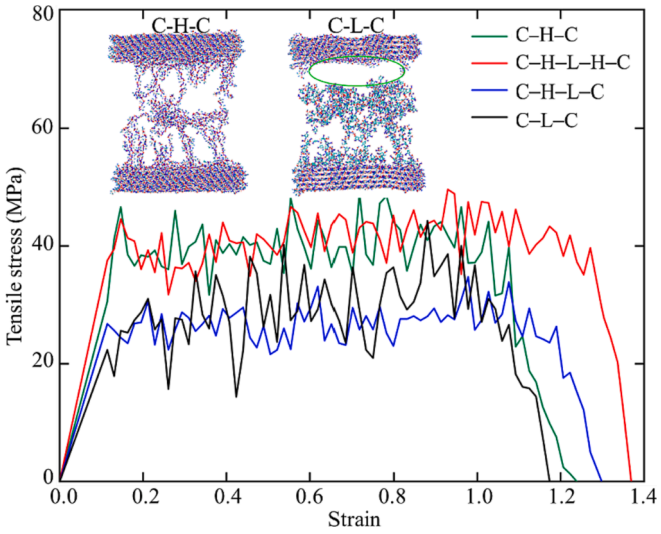

Fig. 13. Tensile stress–strain plots displaying the response of polymer composites sandwiched between layers, with varying compositions and arrangements. The inset images represent snapshots of cellulose-hemicellulose-cellulose (C–H-C) and cellulose-lignin-cellulose (C-L-C) configurations undergoing uniaxial tension [82].

combinations exhibit the highest stiffness, strength, and toughness, whereas cellulose–lignin–cellulose combinations demonstrate the lowest values for these attributes. Careful examination of the deformed structures unveiled that hemicellulose exhibits a propensity to adhere to the cellulose surface, showcasing a robust interfacial interaction. In comparison, interwoven lignin chains were identified as being susceptible to separation from the cellulose bundle, suggesting a relatively mild interaction. Hence, in conjunction with the findings from SMD shear simulations, it was logical to posit that within the coconut endocarp, cellulose bundles are enveloped by hemicellulose, and this composite structure is further embedded in a lignin matrix, given the substantial lignin composition. Furthermore, the density of the amorphous hemicellulose/lignin polymers was demonstrated to exert an impact on the characteristics of the composite.

5. Discussion: Design of artificial materials with controlled nanoscale structure

Establishing a foundational comprehension of the mechanisms through which molecules, components, and intricate structures collaborate to enhance the multifunctionality of biomaterials offers the groundwork for crafting materials, that either emulate the functions of biomaterials or leverage comparable design strategies to confer similar attributes to synthetic materials. It is evident that atomistic modeling plays a pivotal role in achieving this objective. The harmony between structure and function in biomaterials has sparked the design of an extensive array of biomimetic composite materials. A fundamental and pivotal stage in the development of these materials involves discovering a synthetic route to fabricate synthetic counterparts of the biomaterials.

5.1. Nacre-inspired composites

Two-dimensional (2D) films find extensive utility across various domains, encompassing construction, industrial packaging, functional coatings, and flexible device industries [83]. However, conventional 2D films suffer from limited mechanical properties, severely constraining their potential for broader utilization. Motivated by the layered structure of nacre, 2D clay/polymer-based nacre-like films were synthesized, which exhibit improved fracture strength and strain [84]. Nonetheless, this development has consistently focused on centered on emulating the

brick-and-mortar arrangement. The intricate interactions occurring at the interfaces, which have a significant impact on the exceptional mechanical properties of nacre, should not be overlooked. Inspired by the potent electrostatic interactions at the interface between organic and inorganic components [13], the incorporation of ions was pursued to create crosslinking within the 2D layered films through the formation of ionic bonds, by which Significant enhancements were observed in both strength and toughness [85–87].

It has always been the target to develop lighter, stronger, and tougher bulk structural materials. Through pressing, tape casting, and slip-casting techniques, macroscopic SiC and Si_3N_4 tablets were assembled to create layered composites [88]. As in 2D films, interface modification is an efficient enhancement strategy in bulk nacre-inspired materials. A coupling agent of γ-MPS was grafted onto the interface between Al_2O_3 and PMMA, resulting in a hybrid bulk composite. This composite demonstrated extraordinary toughness, exceeding that of either individual component by almost three hundred times (Fig. 14) [38]. A series of sedimentation, drying, and pressing treatments were effectively employed to produce supercrystals composed of oleic acid-coated spherical iron oxide nanoparticles. The application of thermal-induced crosslinking to oleic acid molecules gives rise to a nanocomposite possessing exceptional attributes of hardness, elastic modulus, and strength [89]. In a recent development, drawing inspiration from the mechanism of interlayer energy dissipation involving protein unfolding and entanglement in nacre, a novel approach was undertaken to fabricate materials resembling nacre tablets. This was achieved by utilizing entangled poly(ethylene oxide) (PEO) as the mortar component and incorporating two-dimensional materials such as graphene oxide (GO), graphite nanoplatelets, and boron nitride nanosheets as the sturdy building blocks or "hard bricks." The abundant network of intertwined PEO fibers introduces a multitude of flexible physical connections, enabling increased energy dissipation as the "bricks" separate. This concurrent enhancement of strength and toughness is a distinct characteristic of nacre-like synthetic materials [90]. Nonetheless, efficiently regulating the level of polymer entanglement to meet specific expectations poses a significant challenge.

One may note that the microstructure fabricated by the traditional techniques does not possess the same degree of uniformity as seen in the nacre. However, the pre-programmed additive manufacturing (AM) methods like 3D printing and laser engraving, offer the capability to fabricate lamellar architectures that are notably more uniform and consistent. These methods currently represent the closest approximation to the characteristic structure of nacre [91,92]. Beyond manipulating interface geometry, AM approaches offer the potential to efficiently modify the chemical characteristics of interfaces. A nacre-inspired bulk glass featuring a bowtie-shaped polyurethane (PU) modified interface was successfully produced using laser engraving techniques. The glass composite displayed an extraordinary level of fracture strain, indicating the potential replication of toughening mechanisms akin to those seen in nacre [93].

5.2. Wood-based structural composites

Wood is being explored as a promising alternative to petroleum-based materials, aligning with the goal of fostering sustainability. Leveraging cutting-edge nanotechnology, nanomaterials derived from wood have been fabricated and harnessed for various applications in fields encompassing the environment, energy, and biomedicine [11]. Unlike materials designed with inspiration from nacre, the predominant emphasis in current wood-related research lies in the utilization of wood as a material, rather than exploring the hierarchical structure and interfacial interactions inherent to wood.

Broadly speaking, there exist two approaches for the design of nanomaterials derived from wood: the bottom-up assembly method involves constructing diverse forms from nanocellulose, while the top-down approaches integrate innovative functionalities into already established wood hierarchical structures. Extensive research has been devoted to the separation and extraction of cellulose microfibrils from hemicellulose and lignin, primarily due to cellulose's role as the predominant load-bearing constituent within wood. Utilizing acid hydrolysis, rigid, rod-shaped cellulose nanocrystals were produced, with dimensions ranging from approximately 100 to 300 nm in length and 3 to 5 nm in width [94]. However, it was noted that the acids commonly utilized had a deleterious impact on the thermal stability of cellulose nanocrystals [95]. Indeed, the reported tensile strength of nanocellulose-based fibers and films (~200 MPa) is markedly lower than the strength displayed by individual cellulose nanofibrils (3 ~ 6 GPa) [11].

Considerable advancements have been achieved in enhancing the mechanical properties of cellulose nanofibril-based materials through modulating the structural features of cellulose fibers. As an illustration, in an investigation involving cellulose nanopaper, a notable augmentation in both tensile strength and work of fracture was observed as the degree of polymerization of cellulose molecules increased from 410 to 1100 [96]. Furthermore, an unconventional yet exceptionally favorable scaling law of the cellulose paper was uncovered, demonstrating that smaller dimensions correlate with greater strength and toughness. With a reduction in the mean diameter of cellulose fibers from 27 μm to 11 nm, there is a simultaneous increase in both toughness and ultimate tensile strength [97]. Considering the remarkable mechanical properties and sustainability attributes of cellulose, it is anticipated that a significant amount of cellulose is incorporated into the composite matrix. However, a threshold of 25 % cellulose has hindered the further development due to the cellulose agglomeration [98–100]. Recently, a sustainable structural material has been manufactured by adopting the merits of sophisticated "brick-and-mortar" structure observed in nacre

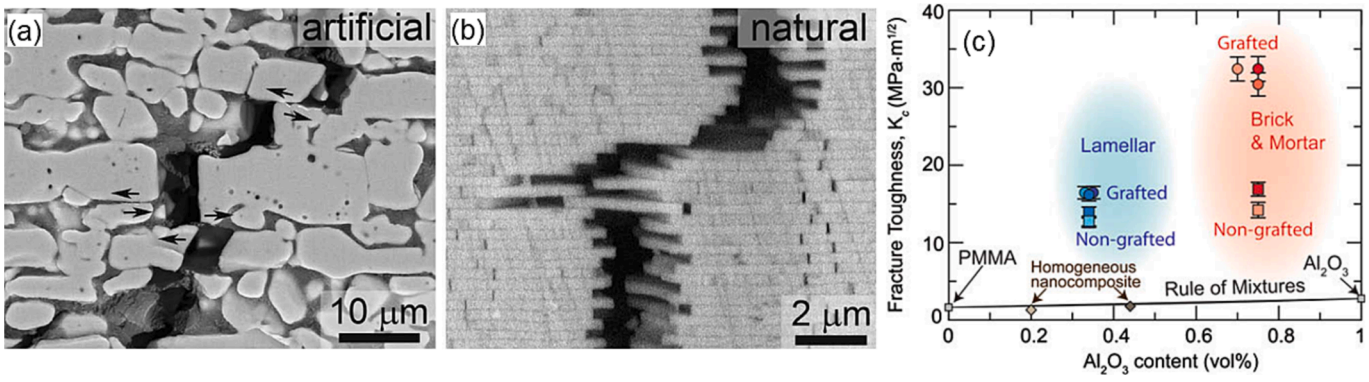

Fig. 14. Fracture of (a) artificial brick-and-mortar material and (b) hydrated nacre. (c) A comparison of the fracture toughness of the Al_2O_3–PMMA composites in both lamella and brick-and-mortar configurations [38].

and the sustainability inherent in cellulose, as shown in Fig. 15 [101]. In this nacre-inspired structure material, the ultrahigh cellulose content (~96.1 %) serves as "brick" and less than 4.0 % hydrophobic polymer (epoxy resin) acts as "mortar". By tailoring the interfaces between cellulose and epoxy resin, i.e., adding Ca^{2+} and oxidation, the fabricated biomimetic material demonstrated a strength of 137 MPa and a toughness of 1.79 $MJ{\cdot}m^{-3}$. This design strategy and manufacturing process demonstrate a minimal environmental footprint, cost-effectiveness, low energy consumption and it could be easily expanded to large-scale applications.

It is notable that the prevailing trend in current research pertaining to wood-based structural materials is focused on reconfiguring cellulose nanofibrils to create materials with elevated performance. The complete translation of the mechanical characteristics of cellulose nanofibrils to macroscopic assembled configurations remains a challenging task [102]. Moreover, there has been relatively less attention given to augmenting the mechanical toughness of bulk wood-based structural materials, despite the potential for leveraging the insights from interfacial interactions unveiled through atomistic modeling [82].

Coconut endocarp-inspired materials design is an emerging area of research and innovation. Given the combination of lightweight yet strong, endocarp is promising for designing new materials that can withstand heavy loads while remaining lightweight. Although there have been extensive experimental studies [70,72], much of the critical structural information and many properties at the nanoscale and the molecular level are missing, many of the structure–function relationships for hierarchically structured coconut endocarp still exist only as a conjecture. Therefore, it is necessary to integrate computer modeling with experimental studies to reveal the structure–property relationships, as well as the role of interfacial interactions at all length scales to advance our understanding of the endocarp's hierarchical design. Integrating computational simulations with experimental studies in a mutually reinforcing manner establishes a fundamental framework for the progression of novel biomimetic materials and structures, enabling their effective integration into real-world technical applications. Computational simulation offers the advantage of dissecting the impact of diverse levels of structural organization, enabling the exploration of structure–property correlations and the identification of pivotal structural components.

Despite substantial dedication and notable progress, the complete replication of the intricate hierarchical structure observed in nature remains a formidable task that exceeds the current capabilities of materials design techniques. There are two important aspects that are challenging and need to be addressed with caution: (1) carefully design the organic–inorganic and organic-organic interfaces and, (2) Create a multilevel hierarchy featuring distinct microstructural designs at each level, aimed at maximizing mechanical performance.

6. Challenges for atomistic modeling

Despite its utility, atomistic modeling, especially in the context of MD simulations, is subject to various limitations. MD relies on empirical potentials to compute interatomic forces. The precision of the anticipated properties derived from MD simulations is heavily contingent on the accuracy of the utilized potential. Some commonly used interatomic potentials for biopolymers and proteins include:

(1) Empirical force fields, such as CHARMM [103,104], AMBER [105,106], GROMACS [107] and PCFF [108]. These potentials enable the study of large and complex biomaterial systems with efficient computation and offering deep insights into the fine-scale dynamic information. However, it is essential to acknowledge that they have limitations, such as limited accuracy and transferability, and inability to capture bond breaking and formation.

(2) Reactive force field (ReaxFF) [109], which is capable of capturing bond-breaking and bond-forming processes during chemical reactions. For example, it was once used to study the pH-drive helical coil transition to random coil [110]. Nevertheless, due to the intense computational cost, ReaxFF is rarely used in the atomistic simulations of biomaterials.

(3) Coarse-graining (CG) modeling is a valuable technique in studying large biomaterial systems [111]. Through using a single bead to represent multiple atoms, CG modeling could significantly reduce the computational burden and meanwhile allow for simulating larger biomaterials over longer timescales. MARTINI is a commonly used potential for biomaterials simulations [112,113]. Yet, CG modeling is restricted by its rough accuracy, in other words, the detailed atomic interaction

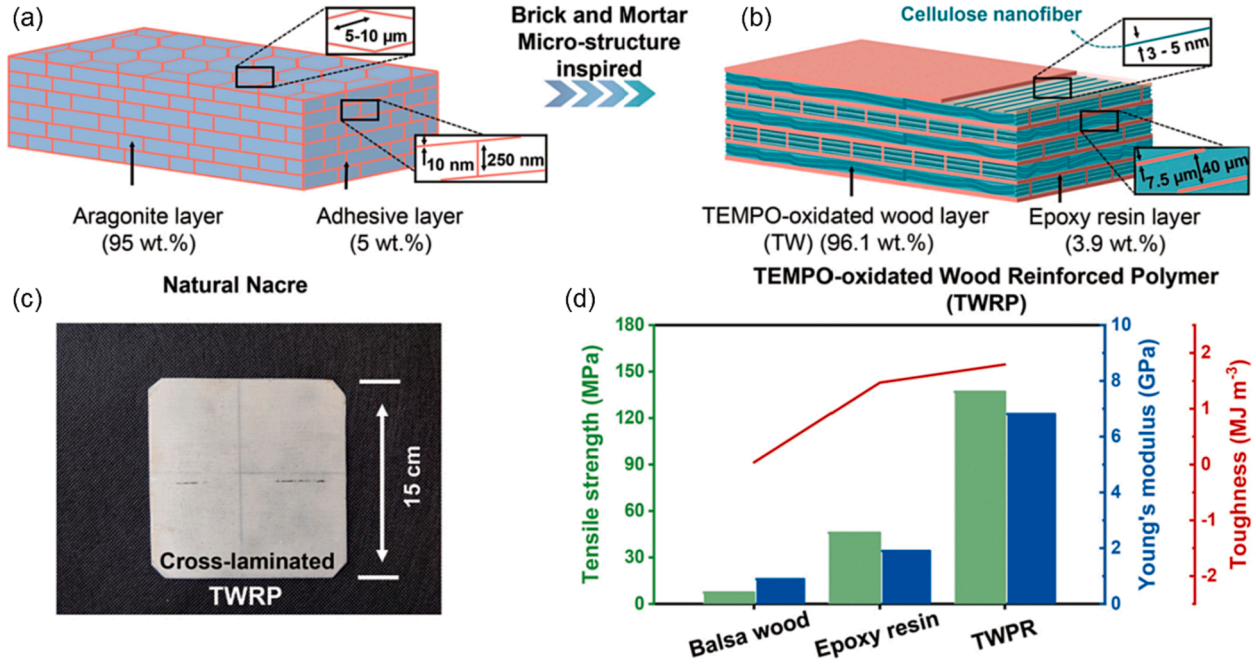

Fig. 15. Schematic configurations of (a) a "brick-and-mortar" structure observed in nacre and (b) cellulose-epoxy resin composite; (c) A photograph of TEMPO-oxidated wood reinforced polymer; (d) Comparison of the normalized tensile strength [101].

information is lost. Therefore, for biomaterials simulations, it is essential to consider the balance between accuracy and computational efficiency when selecting potentials.

Moreover, to ensure accurate capture of atomic vibrations, time steps are set in the femtosecond range, which imposes constraints on the system size, restricting it to submicron dimensions, and limiting the total simulation time to nanoseconds.

7. Outlook and opportunities

With the advancement in computational power and force field development, atomistic modeling will be more accurate, reliable, and applicable to a broader range of biomaterials studies. The synergy between atomistic modeling and experimental empowers us to acquire a more comprehensive understanding of biomaterial behavior. Furthermore, by combining atomistic modeling with other simulation techniques, such as density functional theory, coarse-grained molecular dynamics, and continuum mechanics, a multiscale framework could be established. A step-by-step guide can be summarized as follows: (1) conduct atomistic modeling or gather data from existing MD simulations to understand the detailed atomic structure and properties of biomaterials, as well as obtain the relevant parameters such as bond strength and intermolecular forces; (2) identify key atomic-level structural features that significantly affect the mechanical behavior of the biomaterial, such as heterogeneous structure and crystallographic orientations of minerals; (3) use the atomic-scale information collected from the previous steps to parameterize the constitutive equations in the continuum model, and relate atomic properties to macroscopic material properties; (4) utilize experimental data to calibrate the parameters of the continuum model to ensure accuracy and reliability; (5) develop multiscale modeling technique to bridge the different scales seamlessly. Among the five steps, the last one poses the most significant challenge. Such a multiscale approach will enable the study of biomaterials across multiple length and time scales, providing a more comprehensive view of their properties and the underlying mechanisms.

Eventually, the integration of atomistic modeling with machine learning is expected to further enhance the predictive capabilities of simulations and make them more accurate and efficient. To integrate these approaches, the following steps are expected: (1) conduct a series of MD simulations to generate a dataset that includes information on atomic structures (bond lengths, angles, etc.), mechanical properties (stiffness, strength, toughness, ductility, etc.) and interfacial interactions (forces, bond strengths, etc.). (2) choose a suitable machine learning algorithm based on the nature of the problem and train the modeling using the atomistic dataset; (3) validate the machine learning model using separated atomistic data and tune the model parameters to optimize its predictive accuracy; (4) develop a multiscale framework to integrate them, which could involve using machine learning predictions to inform and accelerate simulations; (5) use the trained machine learning model to predict mechanical properties of biomaterials at different scales. This integration technique has the potential to transfer from one biomaterial to another, which will enhance the generalization of the machine learning model across different materials.

The application of machine learning in studying the mechanical behavior of biomaterials presents numerous exciting opportunities for future materials design. It is essential but with challenges to develop machine learning models that are capable of predicting mechanical properties based on biomaterial composition, structure, and processing parameters. This has the potential to accelerate the design of novel bioinspired materials with tailored mechanical characteristics. Machine learning also provides a way to bridge the gap between atomistic modeling and continuum mechanics. Furthermore, the machine learning method can be used to analyze vast datasets generated from experiments, simulations and literature, which can uncover hidden patterns, correlations and novel insights into the mechanical behavior of biomaterials. Last but not least, machine learning can be used to conduct robustness and sensitivity analysis, exploring how variations in material composition and processing parameters affect mechanical properties. This can contribute to designing bioinspired materials with enhanced properties.

CRediT authorship contribution statement

Ning Zhang: Conceptualization, Funding acquisition, Methodology, Project administration, Supervision, Writing – original draft, Writing – review & editing.

Declaration of Competing Interest

The authors declare that they have no known competing financial interests or personal relationships that could have appeared to influence the work reported in this paper.

Data availability

This is a review article and all the data and figures presented in this article are from previously published work.

Acknowledgments

This work is supported by the National Science Foundation under Award Numbers DMR-2316676 and CMMI-2302981.

References

[1] M. Eder, S. Amini, P. Fratzl, Biological composites—complex structures for functional diversity, Science 362 (6414) (2018) 543–547.
[2] L. Montero de Espinosa, et al., Bioinspired polymer systems with stimuli-responsive mechanical properties, Chemical Reviews 117 (20) (2017) 12851–12892.
[3] D.K. Dubey, V. Tomar, Role of molecular level interfacial forces in hard biomaterial mechanics: a review, Annals of Biomedical Engineering 38 (2010) 2040–2055.
[4] G.M. Luz, J.F. Mano, Biomimetic design of materials and biomaterials inspired by the structure of nacre, Philosophical Transactions of the Royal Society a: Mathematical, Physical and Engineering Sciences 2009 (367) (1893) 1587–1605.
[5] F. Barthelat, et al., On the mechanics of mother-of-pearl: a key feature in the material hierarchical structure, Journal of the Mechanics and Physics of Solids 55 (2) (2007) 306–337.
[6] H. Kakisawa, T. Sumitomo, The toughening mechanism of nacre and structural materials inspired by nacre, Science and Technology of Advanced Materials (2012).
[7] Jackson, A., J.F. Vincent, and R. Turner, *The mechanical design of nacre.* Proceedings of the Royal society of London. Series B. Biological sciences, 1988. **234**(1277): p. 415-440.
[8] D. Verma, K. Katti, D. Katti, Nature of water in nacre: a 2D Fourier transform infrared spectroscopic study, Spectrochimica Acta Part a: Molecular and Biomolecular Spectroscopy 67 (3–4) (2007) 784–788.
[9] J. Sun, B. Bhushan, Hierarchical structure and mechanical properties of nacre: a review, Rsc Advances 2 (20) (2012) 7617–7632.
[10] L. Wagner, et al., Effect of water on the mechanical properties of wood cell walls–results of a nanoindentation study, BioResources 10 (3) (2015) 4011–4025.
[11] F. Jiang, et al., Wood-based nanotechnologies toward sustainability, Advanced Materials 30 (1) (2018) 1703453.
[12] Z. Huang, et al., Uncovering high-strain rate protection mechanism in nacre, Scientific Reports 1 (1) (2011) 148.
[13] N. Zhang, et al., Nanoscale toughening mechanism of nacre tablet, Journal of the Mechanical Behavior of Biomedical Materials 53 (2016) 200–209.
[14] S. Askarinejad, N. Rahbar, Toughening mechanisms in bioinspired multilayered materials, Journal of the Royal Society Interface 12 (102) (2015) 20140855.
[15] Currey, J.D., *Mechanical properties of mother of pearl in tension.* Proceedings of the Royal society of London. Series B. Biological sciences, 1977. **196**(1125): p. 443-463.
[16] X. Shen, et al., Molecular cloning and characterization of lustrin A, a matrix protein from shell and pearl nacre of Haliotis rufescens, Journal of Biological Chemistry 272 (51) (1997) 32472–32481.
[17] I.M. Weiss, et al., Purification and characterization of perlucin and perlustrin, two new proteins from the shell of the mollusc Haliotis laevigata, Biochemical and Biophysical Research Communications 267 (1) (2000) 17–21.
[18] I.M. Weiss, et al., Perlustrin, a Haliotis laevigata (abalone) nacre protein, is homologous to the insulin-like growth factor binding protein N-terminal module of vertebrates, Biochemical and Biophysical Research Communications 285 (2) (2001) 244–249.

[19] L. Treccani, et al., Perlwapin, an abalone nacre protein with three four-disulfide core (whey acidic protein) domains, inhibits the growth of calcium carbonate crystals, Biophysical Journal 91 (7) (2006) 2601–2608.
[20] X. Li, et al., Nanoscale structural and mechanical characterization of a natural nanocomposite material: the shell of red abalone, Nano Letters 4 (4) (2004) 613–617.
[21] R. Wang, et al., Deformation mechanisms in nacre, Journal of Materials Research 16 (9) (2001) 2485–2493.
[22] S. Kotha, Y. Li, N. Guzelsu, Micromechanical model of nacre tested in tension, Journal of Materials Science 36 (2001) 2001–2007.
[23] F. Song, Y. Bai, Effects of nanostructures on the fracture strength of the interfaces in nacre, Journal of Materials Research 18 (8) (2003) 1741–1744.
[24] A.G. Checa, J.H. Cartwright, M.-G. Willinger, Mineral bridges in nacre, Journal of Structural Biology 176 (3) (2011) 330–339.
[25] M.I. Lopez, P.E.M. Martinez, M.A. Meyers, Organic interlamellar layers, mesolayers and mineral nanobridges: Contribution to strength in abalone (Haliotis rufescence) nacre, Acta Biomaterialia 10 (5) (2014) 2056–2064.
[26] M.A. Meyers, et al., Mechanical strength of abalone nacre: role of the soft organic layer, Journal of the Mechanical Behavior of Biomedical Materials 1 (1) (2008) 76–85.
[27] M.A. Meyers, et al., Biological materials: Structure and mechanical properties, Progress in Materials Science 53 (1) (2008) 1–206.
[28] B.A. Wustman, et al., Structure-function studies of the lustrin A polyelectrolyte domains, RKSY and D4, Connective Tissue Research 44 (1) (2003) 10–15.
[29] N. Zhang, Y. Chen, Nanoscale plastic deformation mechanism in single crystal aragonite, Journal of Materials Science 48 (2013) 785–796.
[30] C. Kearney, et al., Nanoscale anisotropic plastic deformation in single crystal aragonite, Physical Review Letters 96 (25) (2006), 255505.
[31] Y.H. Han, et al., Knoop Microhardness Anisotropy of Single-Crystal Aragonite, Journal of the American Ceramic Society 74 (12) (1991) 3129–3132.
[32] F. Barthelat, H. Espinosa, Elastic properties of nacre aragonite tablets. In *Proceedings of the 2003 SEM Annual Conference and Exposition on Experimental and Applied Mechanics*, 2003.
[33] N. Zhang, R. Shahsavari, Balancing strength and toughness of calcium-silicate-hydrate via random nanovoids and particle inclusions: Atomistic modeling and statistical analysis, Journal of the Mechanics and Physics of Solids 96 (2016) 204–222.
[34] N. Zhang, Y. Hong, Y. Chen, Dynamic crack propagation behaviors of calcium carbonate: aragonite, Journal of Materials Science 54 (2019) 2779–2786.
[35] N. Zhang, Y. Chen, Molecular origin of the sawtooth behavior and the toughness of nacre, Materials Science and Engineering: C 32 (6) (2012) 1542–1547.
[36] G.E. Fantner, et al., Sacrificial bonds and hidden length: unraveling molecular mesostructures in tough materials, Biophysical Journal 90 (4) (2006) 1411–1418.
[37] B.L. Smith, et al., Molecular mechanistic origin of the toughness of natural adhesives, fibres and composites, Nature 399 (6738) (1999) 761–763.
[38] M.E. Launey, et al., Designing highly toughened hybrid composites through nature-inspired hierarchical complexity, Acta Materialia 57 (10) (2009) 2919–2932.
[39] M.F. Ashby, et al., The mechanical properties of natural materials. I. Material property charts, Proceedings of the Royal Society of London. Series a: Mathematical and Physical Sciences 1995 (450) (1938) 123–140.
[40] J.F. Vincent, et al., Biomimetics: its practice and theory, Journal of the Royal Society Interface 3 (9) (2006) 471–482.
[41] Y. Li, et al., Optically transparent wood: recent progress, opportunities, and challenges, Advanced Optical Materials 6 (14) (2018) 1800059.
[42] M. Zhu, et al., Highly anisotropic, highly transparent wood composites, Advanced Materials 28 (26) (2016) 5181–5187.
[43] T. Li, Anisotropic, lightweight, strong,, et al., and super thermally insulating nanowood with naturally aligned nanocellulose, Science Advances 4 (3) (2018) eaar3724.
[44] Montanari, C.l,, et al., Transparent wood for thermal energy storage and reversible optical transmittance, ACS Applied Materials & Interfaces 11 (22) (2019) 20465–20472.
[45] Z.-L. Yu, et al., Bioinspired polymeric woods, Science Advances 4 (8) (2018) eaat7223.
[46] Y. He, et al., Bleached wood supports for floatable, recyclable, and efficient three dimensional photocatalyst, Catalysts 9 (2) (2019) 115.
[47] W. Huang, et al., Multiscale toughening mechanisms in biological materials and bioinspired designs, Advanced Materials 31 (43) (2019) 1901561.
[48] S. Wang, A. Lu, L. Zhang, Recent advances in regenerated cellulose materials, Progress in Polymer Science 53 (2016) 169–206.
[49] F. Chen, et al., Mesoporous, three-dimensional wood membrane decorated with nanoparticles for highly efficient water treatment, Acs Nano 11 (4) (2017) 4275–4282.
[50] C. Zhang, et al., *Hygromechanical mechanisms of wood cell wall revealed by molecular modeling and mixture rule analysis.* Science, Advances 7 (37) (2021) eabi8919.
[51] Fernandes, A.N., et al., *Nanostructure of cellulose microfibrils in spruce wood.* Proceedings of the National Academy of Sciences, 2011. **108**(47): p. E1195-E1203.
[52] J.F. Vincent, From cellulose to cell, Journal of Experimental Biology 202 (23) (1999) 3263–3268.
[53] Q. Deng, S. Li, Y. Chen, Mechanical properties and failure mechanism of wood cell wall layers, Computational Materials Science 62 (2012) 221–226.
[54] C. Altaner, M. Jarvis, Modelling polymer interactions of the 'molecular Velcro'type in wood under mechanical stress, Journal of Theoretical Biology 253 (3) (2008) 434–445.
[55] N. Zhang, et al., Cellulose-hemicellulose interaction in wood secondary cell-wall, Modelling and Simulation in Materials Science and Engineering 23 (8) (2015) 085010.
[56] K. Jin, Z. Qin, M.J. Buehler, Molecular deformation mechanisms of the wood cell wall material, Journal of the Mechanical Behavior of Biomedical Materials 42 (2015) 198–206.
[57] I. Burgert, Exploring the micromechanical design of plant cell walls, American Journal of Botany 93 (10) (2006) 1391–1401.
[58] A. Reiterer, et al., Experimental evidence for a mechanical function of the cellulose microfibril angle in wood cell walls, Philosophical Magazine A 79 (9) (1999) 2173–2184.
[59] L. Mishnaevsky Jr, H. Qing, Micromechanical modelling of mechanical behaviour and strength of wood: State-of-the-art review, Computational Materials Science 44 (2) (2008) 363–370.
[60] F.K. Wittel, G. Dill-Langer, B.-H. Kröplin, Modeling of damage evolution in soft-wood perpendicular to grain by means of a discrete element approach, Computational Materials Science 32 (3–4) (2005) 594–603.
[61] A. Da Silva, S. Kyriakides, Compressive response and failure of balsa wood, International Journal of Solids and Structures 44 (25–26) (2007) 8685–8717.
[62] R.O. Ritchie, The conflicts between strength and toughness, Nature Materials 10 (11) (2011) 817–822.
[63] W. Wagermaier, K. Klaushofer, P. Fratzl, Fragility of bone material controlled by internal interfaces, Calcified Tissue International 97 (2015) 201–212.
[64] E. Flores-Johnson, et al., Microstructure and mechanical properties of hard Acrocomia mexicana fruit shell, Scientific Reports 8 (1) (2018) 9668.
[65] C. Lauer, et al., Strength-size relationships in two porous biological materials, Acta Biomaterialia 77 (2018) 322–332.
[66] J. Chen, B. Young, B. Uy, Behavior of high strength structural steel at elevated temperatures, Journal of Structural Engineering 132 (12) (2006) 1948–1954.
[67] V.R. Salvini, V.C. Pandolfelli, D. Spinelli, Mechanical properties of porous ceramics, Recent Adv. Porous Ceram 34 (2018) 171–199.
[68] P.G. Dixon, L.J. Gibson, The structure and mechanics of Moso bamboo material, Journal of the Royal Society Interface 11 (99) (2014) 20140321.
[69] M. Borrega, L.J. Gibson, Mechanics of balsa (Ochroma pyramidale) wood, Mechanics of Materials 84 (2015) 75–90.
[70] B. Gludovatz, et al., Multiscale structure and damage tolerance of coconut shells, Journal of the Mechanical Behavior of Biomedical Materials 76 (2017) 76–84.
[71] J. Knippers, K.G. Nickel, T. Speck, Biomimetic research for architecture and building construction, Springer International Publishing, Switzerland, 2016.
[72] S. Schmier, N. Hosoda, T. Speck, Hierarchical structure of the Cocos nucifera (coconut) endocarp: Functional morphology and its influence on fracture toughness, Molecules 25 (1) (2020) 223.
[73] E.A. Zimmermann, et al., Mechanical adaptability of the Bouligand-type structure in natural dermal armour, Nature Communications 4 (1) (2013) 2634.
[74] Zimmermann, E.A., et al., *Age-related changes in the plasticity and toughness of human cortical bone at multiple length scales.* Proceedings of the National Academy of Sciences, 2011. **108**(35): p. 14416-14421.
[75] K.J. Koester, J. Ager Iii, R. Ritchie, The true toughness of human cortical bone measured with realistically short cracks, Nature Materials 7 (8) (2008) 672–677.
[76] R.K. Nalla, J.H. Kinney, R.O. Ritchie, Mechanistic fracture criteria for the failure of human cortical bone, Nature Materials 2 (3) (2003) 164–168.
[77] R.K. Nalla, et al., Mechanistic aspects of fracture and R-curve behavior in human cortical bone, Biomaterials 26 (2) (2005) 217–231.
[78] C. Lu, et al., The mystery of coconut overturns the crashworthiness design of composite materials, International Journal of Mechanical Sciences 168 (2020) 105244.
[79] A. Demirbaş, Estimating of structural composition of wood and non-wood biomass samples, Energy Sources 27 (8) (2005) 761–767.
[80] V. Mendu, et al., Identification and thermochemical analysis of high-lignin feedstocks for biofuel and biochemical production, Biotechnology for Biofuels 4 (1) (2011) 1–14.
[81] S. Zhao, et al., Changes in lignin content and activity of related enzymes in the endocarp during the walnut shell development period, Horticultural Plant Journal 2 (3) (2016) 141–146.
[82] S. Mazumder, N. Zhang, Cellulose–Hemicellulose–Lignin Interaction in the Secondary Cell Wall of Coconut Endocarp, Biomimetics 8 (2) (2023) 188.
[83] R. Cruz-Silva, M. Endo, M. Terrones, Graphene oxide films, fibers, and membranes, Nanotechnology Reviews 5 (4) (2016) 377–391.
[84] Z. Tang, et al., Nanostructured artificial nacre, Nature Materials 2 (6) (2003) 413–418.
[85] K. Chen, et al., Strong and tough layered nanocomposites with buried interfaces, ACS Nano 10 (4) (2016) 4816–4827.
[86] K. Chen, et al., A general bioinspired, metals-based synergic cross-linking strategy toward mechanically enhanced materials, ACS Nano 11 (3) (2017) 2835–2845.
[87] S. Wan, et al., Superior fatigue resistant bioinspired graphene-based nanocomposite via synergistic interfacial interactions, Advanced Functional Materials 27 (10) (2017) 1605636.
[88] J. Wang, Q. Cheng, Z. Tang, Layered nanocomposites inspired by the structure and mechanical properties of nacre, Chemical Society Reviews 41 (3) (2012) 1111–1129.
[89] A. Dreyer, et al., Organically linked iron oxide nanoparticle supercrystals with exceptional isotropic mechanical properties, Nature Materials 15 (5) (2016) 522–528.

[90] L. Wang, et al., Superior Strong and Tough Nacre-Inspired Materials by Interlayer Entanglement, Nano Letters 23 (8) (2023) 3352–3361.
[91] R. Yadav, et al., Review on 3D prototyping of damage tolerant interdigitating brick arrays of nacre, Industrial & Engineering Chemistry Research 56 (38) (2017) 10516–10525.
[92] L.-B. Mao, et al., Synthetic nacre by predesigned matrix-directed mineralization, Science 354 (6308) (2016) 107–110.
[93] S.M.M. Valashani, F. Barthelat, A laser-engraved glass duplicating the structure, mechanics and performance of natural nacre, Bioinspiration & Biomimetics 10 (2) (2015) 026005.
[94] L. Chen, et al., Tailoring the yield and characteristics of wood cellulose nanocrystals (CNC) using concentrated acid hydrolysis, Cellulose 22 (2015) 1753–1762.
[95] M. Roman, W.T. Winter, Effect of sulfate groups from sulfuric acid hydrolysis on the thermal degradation behavior of bacterial cellulose, Biomacromolecules 5 (5) (2004) 1671–1677.
[96] M. Henriksson, et al., Cellulose nanopaper structures of high toughness, Biomacromolecules 9 (6) (2008) 1579–1585.
[97] Zhu, H., et al., *Anomalous scaling law of strength and toughness of cellulose nanopaper*. Proceedings of the National Academy of Sciences, 2015. **112**(29): p. 8971-8976.
[98] F. Ansari, L.A. Berglund, Toward semistructural cellulose nanocomposites: the need for scalable processing and interface tailoring, Biomacromolecules 19 (7) (2018) 2341–2350.
[99] S. Ling, et al., Biopolymer nanofibrils: Structure, modeling, preparation, and applications, Progress in Polymer Science 85 (2018) 1–56.
[100] X. Yang, et al., Surface and interface engineering for nanocellulosic advanced materials, Advanced Materials 33 (28) (2021) 2002264.
[101] H. Sun, et al., Ultrahigh content cellulose reinforced sustainable structural materials enabled by a nacre-inspired strategy, Industrial Crops and Products 180 (2022) 114749.
[102] S. Wang, et al., Super-strong, super-stiff macrofibers with aligned, long bacterial cellulose nanofibers, Advanced Materials 29 (35) (2017) 1702498.
[103] O. Guvench, et al., Additive empirical force field for hexopyranose monosaccharides, Journal of Computational Chemistry 29 (15) (2008) 2543–2564.
[104] E.R. Hatcher, O. Guvench, A.D. MacKerell Jr, CHARMM additive all-atom force field for acyclic polyalcohols, acyclic carbohydrates, and inositol, Journal of Chemical Theory and Computation 5 (5) (2009) 1315–1327.
[105] D.A. Case, et al., The Amber biomolecular simulation programs, Journal of Computational Chemistry 26 (16) (2005) 1668–1688.
[106] J. Wang, et al., Development and testing of a general amber force field, Journal of Computational Chemistry 25 (9) (2004) 1157–1174.
[107] H.J. Berendsen, D. van der Spoel, R. van Drunen, GROMACS: A message-passing parallel molecular dynamics implementation, Computer Physics Communications 91 (1–3) (1995) 43–56.
[108] H. Sun, et al., An ab initio CFF93 all-atom force field for polycarbonates, Journal of the American Chemical Society 116 (7) (1994) 2978–2987.
[109] A.C. Van Duin, et al., ReaxFF: a reactive force field for hydrocarbons, The Journal of Physical Chemistry A 105 (41) (2001) 9396–9409.
[110] Golkaram, M., *Application of Reactive Molecular Dynamics in Biomaterial Science and Computational Biology*. 2014.
[111] T. Bereau, M. Deserno, Generic coarse-grained model for protein folding and aggregation, Biophysical Journal 96 (3) (2009) 405a.
[112] López, C.s.A, et al., MARTINI coarse-grained model for crystalline cellulose microfibers, The Journal of Physical Chemistry B 119 (2) (2015) 465–473.
[113] Z. Yu, D. Lau, Development of a coarse-grained α-chitin model on the basis of MARTINI forcefield, Journal of Molecular Modeling 21 (2015) 1–9.